Euro. Jnl of Applied Mathematics (2004), *vol.* 15, *pp.* 315–327.
DOI: 10.1017/S0956792504005509 Printed in the United Kingdom

On bubble rising in a Hele–Shaw cell filled with a non-Newtonian fluid

A. N. ALEXANDROU[1], V. M. ENTOV[2], S. S. KOLGANOV[3] and N. V. KOLGANOVA[3]

[1] *Department of Mechanical and Manufacturing Engineering, University of Cyprus, Nicosia, Cyprus*
[2] *Institute for Problems in Mechanics, Russian Academy of Science, 101-1, pr. Vernadskogo, Moscow, 119526, Russia*
email: entov@ipmnet.ru
[3] *Russian Gubkin State Oil and Gas University, 65, Leninsky pr., Moscow, 117917, Russia*

(*Received 21 October 2001; revised 19 September 2003*)

The problem of a bubble rising due to buoyancy in a Hele–Shaw cell filled with a viscous fluid is a classical free-boundary problem first posed and solved by Saffman & Taylor [11]. In fact, due to linearity of the flow equations the problem is reduced to that of a bubble transported by uniform fluid flow. Saffman and Taylor provided explicit expressions for the bubble shape. Steady propagation of bubbles and fingers in a Hele–Shaw cell filled with a nonlinearly-viscous fluid was studied by Alexandrou & Entov [1]. In Alexandrou & Entov [1], it was shown that for a nonlinearly viscous fluid the problem of a rising bubble cannot be reduced to that of a steadily transported bubble, and should be treated separately. This note presents a solution of the problem following the general framework suggested in Alexandrou & Entov [1]. The hodograph transform is used in combination with finite-difference and collocation techniques to solve the problem. Results are presented for the cases of a Bingham and power-law fluids.

1 The problem formulation

We shall consider a steady-state rising of an "air bubble" through a vertical Hele–Shaw cell filled with a nonlinearly-viscous non-Newtonian fluid at rest at infinity. The air viscosity, density and capillary pressure across the air-fluid interface are assumed to be negligible. Then using the usual approximation for Hele–Shaw flow we have the following equations for the velocity $\mathbf{w}(x, y)$ and pressure $p(x, y)$ fields within the cell:

$$\operatorname{div} \mathbf{w} = 0, \tag{1.1}$$

$$-\nabla(H + x) = \Phi(w)\frac{\mathbf{w}}{w}, \quad w = |\mathbf{w}|, \quad H = \frac{p}{\rho g}. \tag{1.2}$$

Here, $\mathbf{w}$ is the fluid velocity averaged across the cell gap, p is the pressure, H is the hydraulic head, ρ is the fluid density, g is the component of acceleration due to gravity along the negative x direction. The non-dimensional function $\Phi(w)$ expresses the flow rule

through the thin gap. In particular,

$$\Phi(w) = \frac{12\eta w}{b^2\rho g} \tag{1.3}$$

for a Newtonian fluid of viscosity η (b is the Hele–Shaw cell gap),

$$\Phi(w) = Gw^s, \quad G = \frac{2^{s+1}(2s+1)^s K}{s^s b^{s+1}}, \quad K = const \tag{1.4}$$

for a power-law nonlinearly-viscous fluid, and

$$\Phi(w) = \frac{12\eta}{b^2\rho g}(w + \gamma) \tag{1.5}$$

for a Bingham (visco-plastic) fluid. The reasons for using the simplified expression (1.5) instead of more precise Buckingham formula (cf. Reiner [9]) are presented in Alexandrou & Entov [1]. Essentially, they consist in that flow rule for real viscoplastic fluids in narrow slits can be equally well approximated by the Buckingham formula and its simplified counterpart. More recent discussion of the proper form of the averaged flow law in a Hele–Shaw cell can be found elsewhere [5, 7, 12]. Much more important, however, the same equations describe flow of non-Newtonian (respectively, power-law and Bingham) fluids through porous media (see Barenblatt *et al.* [2], Bernardiner & Entov [3] and Bernardiner *et al.* [4]), and all the results and techniques developed here apply to porous media flows as well; more than that, most of techniques can be extended to other forms of relation between the average local velocity and the hydraulic head gradient $\Phi(w)$.

We assume that the fluid within the "air bubble" is both inviscid and weightless. Therefore, the pressure is constant throughout the bubble, and hence on its boundary ∂D:

$$p(x, y) = 0, \quad \text{or} \quad H = x, \quad (x, y) \in \partial D. \tag{1.6}$$

On the other hand, the steady rising bubble does not change its shape, and propagates as a solid body. We introduce the stream function $\psi(x, y)$. Then

$$\psi(x, y) = Vy, \quad (x, y) \in \partial D, \tag{1.7}$$

V being the bubble velocity. We will confine our analysis to the case of a Hele–Shaw cell of an infinite extent (or an infinite width). Then the last boundary condition is that the fluid far from the bubble is at rest:

$$w(x, y) \to 0, \quad x^2 + y^2 \to \infty. \tag{1.8}$$

It looks plausible (from a physical "common sense" argument) that for specified properties of the fluid, the shape and velocity of the bubble will depend only on the bubble size characterized, say, by the bubble area S. However, it turns out that for given fluid properties, gravity force and the bubble size (area), even in the Saffman–Taylor case there exists one-parameter family of solutions differing in the bubble rising velocity and shape (the aspect ratio). In fact, these bubbles have oval shapes of different elongation. The same property applies also to the problems considered in this note.

https://doi.org/10.1017/S0956792504005509 Published online by Cambridge University Press

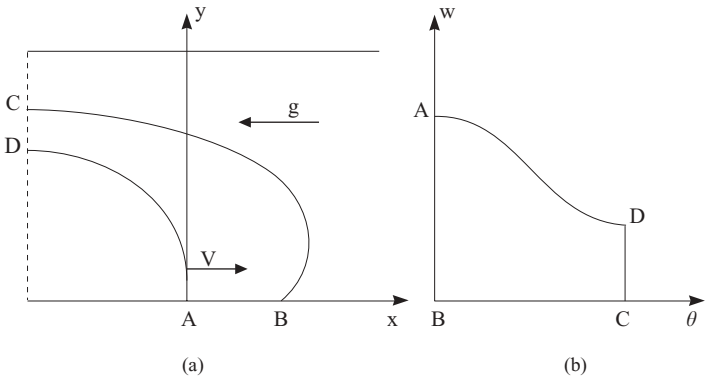

FIGURE 1. Schematic of flow in physical plane (*a*) and in hodograph plane (*b*).

In the case of a Bingham (plastic) fluid, we expect also that the flow will be confined to a finite annular domain between the bubble and an external stagnant zone (cf. Figure 1(a)), within which $w \equiv 0$. In this case, the stagnant zone boundary is another unknown free boundary to be determined.

2 Hodograph transform

The key to effective solution of the problem stated above is using the hodograph transform, which simultaneously transforms free boundaries into known ones and reduces nonlinear flow equations to linear ones. This technique, originating from gas dynamics, proved to be rather effective in the problems of flows through porous media following the seepage law with limiting pressure gradient [2]–[4]. Below, we summarize briefly the main necessary relations. We choose the velocity magnitude w and angle θ between the x-axis and the velocity vector $\mathbf{w}$ as new independent variables, and the stream function ψ, the hydraulic head H, and the physical coordinates x and y as new unknowns.

The functions $H(w,\theta)$ and $\psi(w,\theta)$ satisfy the following set of equations:

$$\frac{\partial H}{\partial \theta} = -\frac{\Phi^2(w)}{w\Phi'(w)}\frac{\partial \psi}{\partial w}; \qquad \frac{\partial H}{\partial w} = \frac{\Phi(w)}{w^2}\frac{\partial \psi}{\partial \theta}. \tag{2.1}$$

Equations (2.1) can be reduced to an elliptic equation for the stream function ψ:

$$\frac{\partial}{\partial w}\left(\frac{\Phi^2(w)}{w\Phi'(w)}\frac{\partial \psi}{\partial w}\right) + \frac{\Phi(w)}{w^2}\frac{\partial^2 \psi}{\partial \theta^2} = 0. \tag{2.2}$$

The coordinates in the physical plane are expressed in terms of $H(w,\theta)$ and $\psi(w,\theta)$ [1]–[3] by integration of the relation

$$dz = dx + i dy = e^{i\theta}\left(-\frac{dH}{\Phi(w)} + i\frac{d\psi}{w}\right). \tag{2.3}$$

Using relations (2.3), boundary conditions (1.6) and (1.7) at the surface of the bubble are

https://doi.org/10.1017/S0956792504005509 Published online by Cambridge University Press

reduced to

$$\frac{dH}{\rho g} = -\cos\theta \frac{dH}{\Phi(w)} - \sin\theta \frac{d\psi}{w}; \quad \frac{d\psi}{V} = -\sin\theta \frac{dH}{\Phi(w)} + \cos\theta \frac{d\psi}{w}. \tag{2.4}$$

Requiring that these linear simultaneous equations have a non-trivial solution for $d\psi$, dH, one finds that the following relation should hold along the boundary:

$$R(w) \equiv \cos\theta(w) = \frac{\rho g V - w\Phi(w)}{\rho g w - V\Phi(w)}. \tag{2.5}$$

This equation determines the shape of the part of the boundary in the hodograph plane corresponding to the surface of the bubble. This shape explicitly depends on the specific form of the "flow rule" $\Phi(w)$ expressing the dependence of the hydraulic head gradient on the flow velocity. Now, introducing into (2.4)

$$dH = \frac{\partial H}{\partial w} dw + \frac{\partial H}{\partial \theta} d\theta; \quad d\psi = \frac{\partial \psi}{\partial w} dw + \frac{\partial \psi}{\partial \theta} d\theta, \tag{2.6}$$

and expressing the derivatives $\partial H/\partial w$ and $\partial H/\partial \theta$ in terms of $\partial \psi/\partial w$ and $\partial \psi/\partial \theta$, we have the following boundary conditions along the bubble boundary in the hodograph plane:

$$\text{along} \quad AB \quad \text{and} \quad BC, \quad \psi = 0; \quad \text{along} \quad CD, \quad H = 0 \quad \left(\text{or} \quad \frac{\partial \psi}{\partial \theta} = 0\right); \tag{2.7}$$

$$\text{at the point} \quad D, \quad \psi = \lambda V; \quad \text{along} \quad AD, \quad A(w,\theta)\frac{\partial \psi}{\partial w} + B(w,\theta)\frac{\partial \psi}{\partial \theta} = 0. \tag{2.8}$$

Here, λ is the maximum value of the bubble width, $0 \leqslant \theta \leqslant \pi$, $0 \leqslant w \leqslant V$, and

$$A(w,\theta) = \left(w - VR + \frac{V\Phi(w)}{\Phi'(w)}\frac{dR}{dw}\right)\sqrt{1 - R^2(w)}, \tag{2.9}$$

$$B(w,\theta) = \frac{V(1 - R^2(w))}{w} + (VR - w)\frac{dR}{dw}. \tag{2.10}$$

Notice that the conditions (2.7)–(2.10) were derived in Alexandrou & Entov [1]; however, there is a typo error in Alexandrou & Entov [1].

Finally, in the case of flow of a visco-plastic fluid (flow with a limiting pressure gradient) the part of the boundary

$$w = 0, \quad 0 \leqslant \theta \leqslant \pi, \tag{2.11}$$

corresponds to the boundary of the stagnant zone.

So in our case (2.2) should be solved in the known domain of the hodograph plane which is shown in Figure 1 with boundary conditions (2.7)–(2.10).

3 Solution of the problem in the hodograph plane

So far, we have not specified the concrete form of the function $\Phi(w)$ describing rheological behavior of the fluid. In this paper, two typical functions forms $\Phi(w)$ are used that

https://doi.org/10.1017/S0956792504005509 Published online by Cambridge University Press

correspond to a visco-plastic (Bingham) flow, or a flow with limiting pressure gradient, [1]–[3]

$$\Phi(w) = \frac{12\eta}{b^2}(w+\gamma), \quad w > 0; \quad \Phi(0+) = \frac{12\eta\gamma}{b^2} > 0, \tag{3.1}$$

γ being the liquid rheological parameter, and the power law (Ostwald-de-Waele) fluid, [2, 3]:

$$\Phi(w) = Cw^s, \quad s > 0. \tag{3.2}$$

Let us consider these two cases in more detail.

3.1 Flow with limiting pressure gradient

Using expression (3.1) for $\Phi(w)$, equation (2.2) becomes

$$w(w+\gamma)\frac{\partial^2\psi}{\partial w^2} + (w-\gamma)\frac{\partial\psi}{\partial w} + \frac{\partial^2\psi}{\partial\theta^2} = 0. \tag{3.3}$$

Two techniques were used for solving (3.3), namely, a numerical finite difference technique and a version of the collocation technique to be described in more detail later.

Equation (2.5) implies the following inequality that bounds the range of variation of problem parameters: $\gamma \leqslant V_* \leqslant V$; $V_* = \rho g b^2/12\eta$. A version of a stabilization technique was used to solve the steady-state problem formulated above. We first rewrite (3.3) as:

$$w(w+\gamma)\frac{\partial^2\psi}{\partial w^2} + (w-\gamma)\frac{\partial\psi}{\partial w} + \frac{\partial^2\psi}{\partial\theta^2} = \frac{\partial\psi}{\partial t}. \tag{3.4}$$

This non-steady-state equation was solved using the well-developed numerical technique of alternating directions [13]. At large values of t, the solution stabilizes to that of the steady-state equation (3.3).

The numerical grid in the domain $0 \leqslant \theta \leqslant \pi$, $0 \leqslant w \leqslant V$ in the hodograph plane consists of equidistant mesh points along θ-axis. The mesh step along w is variable, so that the boundary mesh points are located on the curvilinear part of the boundary AD (Figure 1(b)).

When the stream function values are found in all mesh points, the flow pattern in the physical plane is determined using (1.6), (1.7), (2.3) and (2.1), assuming $x_A = 0$, $y_A = 0$ (i.e. choosing the bubble tip for the origin). In particular, for the bubble boundary we have

$$x(\theta) = \int_0^\theta \frac{1}{w}\left[\left((w+\gamma)\cos\theta + \frac{\sin^2\theta}{R_w}\right)\frac{\partial\psi}{\partial w} + \sin\theta\left(\frac{\cos\theta}{wR_w} - 1\right)\frac{\partial\psi}{\partial\theta}\right]d\theta, \tag{3.5}$$

$$y(\theta) = \frac{\psi}{V}. \tag{3.6}$$

Here $w = w(\theta)$ are values corresponding to the bubble boundary,

$$\psi = \psi(w(\theta),\theta), \quad R_w = \frac{dR}{dw}(w(\theta)), \quad \frac{\partial\psi}{\partial w} = \frac{\partial\psi}{\partial w}(w(\theta),\theta), \quad \frac{\partial\psi}{\partial\theta} = \frac{\partial\psi}{\partial\theta}(w(\theta),\theta). \tag{3.7}$$

https://doi.org/10.1017/S0956792504005509 Published online by Cambridge University Press

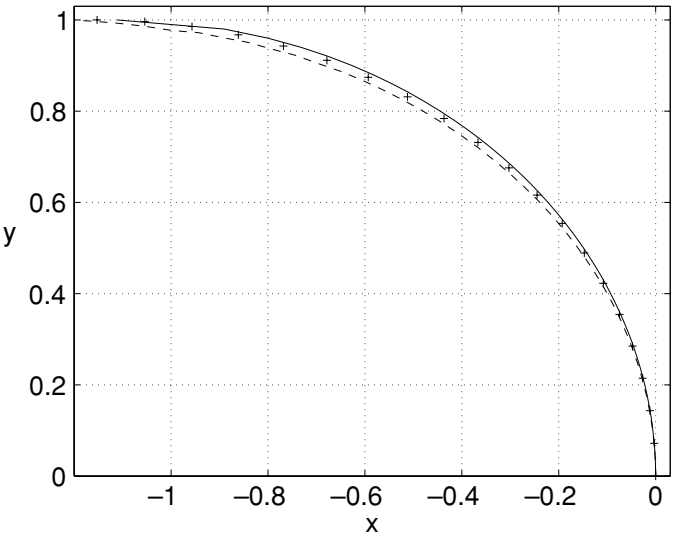

FIGURE 2. The bubble boundary for $V = 1$, $V_* = 0.9$ predicted by the Saffman–Taylor theory (solid line), the finite difference technique with $\gamma = 0.005$ (broken line) and the collocation technique (crosses) in dimensionless coordinates X and Y.

Location and size of the stagnant zone is determined from (2.3) as

$$x_B = \int_0^V \frac{1}{w^2}\frac{\partial \psi}{\partial \theta}(w,0)\,dw, \quad y_B = 0 \tag{3.8}$$

to find the position of the initial point B, and

$$x(\theta) + iy(\theta) = \lim_{w\to 0}\int_0^\theta e^{i\theta}\frac{w+\gamma}{w}\frac{\partial \psi}{\partial w}(w,\theta)\,d\theta + x_B, \tag{3.9}$$

to determine the shape of the boundary of the stagnant zone.

To test the validity of the numerical technique, it was first applied to several well-studied free boundary problems, namely the problem of the Saffman–Taylor finger propagating steadily in a Hele–Shaw cell [1, 10] and seepage flow of a Bingham fluid [2]–[4]. Numerical results agree rather well with the analytical solution for the bubble in the cases when the analytical solution is available (Figure 2). We recall, that the Saffman–Taylor solution for the steadily propagating bubble is:

$$x = \frac{2}{\pi}\frac{U-1}{U}\tanh^{-1}\left(\sin^2\frac{\lambda\pi U}{2} - \cos^2\frac{\lambda\pi U}{2}tg^2\frac{y\pi U}{2}\right)^{1/2}, \tag{3.10}$$

where $U = 1 + V/V_*$; $V_* = \rho g b^2/12\eta$.

3.2 Numerical-analytical solution for the flow with limiting pressure gradient

In our case, the stream function in the hodograph plane satisfies (3.3) with $\Phi(w) = (w+\gamma)/V_*$ and vanishes at the boundaries $w = 0$, and $\theta = 0$ and $\theta = \pi$. Therefore, this

https://doi.org/10.1017/S0956792504005509 Published online by Cambridge University Press

solution can be represented by a Fourier series expansion involving a particular family of hypergeometric functions (cf. Bernadiner & Entov [3]; see also Goldstein & Entov [6]). We first introduce a new dimensionless velocity variable u:

$$u = \frac{w}{\gamma}, \quad g^0 = \frac{\rho g}{\gamma}, \quad V^0 = \frac{V}{\gamma}, \quad A^0(u,\theta) = \frac{A(w,\theta)}{\gamma}, \quad B^0(u,\theta) = B(w,\theta). \tag{3.11}$$

Then (3.3) becomes

$$u(u+1)\frac{\partial^2\psi}{\partial u^2} + (u-1)\frac{\partial\psi}{\partial u} + \frac{\partial^2\psi}{\partial\theta^2} = 0. \tag{3.12}$$

Here, $\psi(u,\theta)$ should satisfy the following boundary conditions:

$$\psi = 0 \quad \text{along} \quad AB \quad \text{and} \quad BC, \tag{3.13}$$

$$\frac{\partial\psi}{\partial\theta} = 0 \quad \text{along} \quad CD. \tag{3.14}$$

The general solution of this problem is given by the series

$$\psi(u,\theta) = \sum_{n=1}^{\infty} C_n u^2 F(2-\alpha_n, 2+\alpha_n, 3, -u)\sin\alpha_n\theta; \tag{3.15}$$

$$H(u,\theta) = \sum_{n=1}^{\infty} 2C_n\alpha_n^{-1} F(-\alpha_n, \alpha_n, 2, -u)\cos\alpha_n\theta, \tag{3.16}$$

where $\alpha_n = n - \frac{1}{2}$, C_n are unknown coefficients, F is a hypergeometric function [8]. To evaluate the function $F = F(a,b,c,z)$ a standard series development was used:

$$F(a,b,c,z) = \sum_{k=0}^{\infty} \frac{(a)_k(b)_k}{(c)_k k!} z^k, \quad |z| < 1, \quad (\phi)_k = \frac{\Gamma(\phi+k)}{\Gamma(\phi)}. \tag{3.17}$$

However, this diverges beyond a circle of unit radius, so that the Kummer formulas (cf. Lebedev [8]) which provide analytic continuation of F on the complex plane with a slit along $1 \leqslant z \leqslant \infty$ were used:

$$F(a,b,c,z) = (1-z)^{-b} F\left(c-a, b; c; \frac{z}{z-1}\right). \tag{3.18}$$

Thus, the problem of determination of $\psi(u,\theta)$ is reduced to finding of the coefficients C_n. This is done using the boundary condition along the curvilinear part of the boundary AD that assumes the form

$$A^0(u,\theta)\frac{\partial\psi}{\partial u} + B^0(u,\theta)\frac{\partial\psi}{\partial\theta} = 0, \quad \psi(g^0 - 1, \pi) = \lambda V, \tag{3.19}$$

and a point-by-point collocation method. We select a finite number N of terms of the series (3.15), (3.16) and (3.18). Choosing a set of points θ_i, $i = 0..N$ in the interval $[0,\pi]$ and substituting values of the functions A^0, B^0 and derivatives $\partial\psi/\partial u$, $\partial\psi/\partial\theta$ at the boundary points $(\theta_i, u(\theta_i))$ into (3.8), we arrive at a linear system of equation for C_n. After that using (3.8), (3.9) we recover coordinates of the bubble boundary in the physical plane.

https://doi.org/10.1017/S0956792504005509 Published online by Cambridge University Press

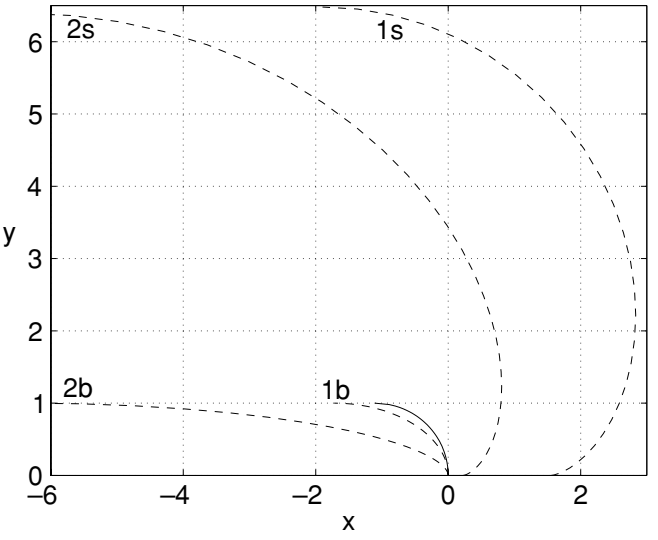

FIGURE 3. The shapes of bubbles (1b, 2b) and stagnant zones (1s, 2s) for $V = 1$, $V_* = 0.9$. Curves 1b and 1s show the results derived by the collocation technique with $\gamma = 0.1$, 2b and 2s – with $\gamma = 0.5$; the Saffman-Taylor solution is shown as a solid line.

In our case, the location of the initial point B of the stagnant zone is given by the expression

$$x_B = \frac{1}{\gamma}\int_0^V \sum_{n=1}^{N} C_n \alpha_n F(2-\alpha_n, 2+\alpha_n, 3, -u)\, du, \qquad y_B = 0. \tag{3.20}$$

and the boundary of the stagnant zone is described by the relations:

$$x(\theta) = x_B - \frac{1}{\gamma}\sum_{n=1}^{N} C_n \left(\frac{\cos(\alpha_n - 1)\theta}{\alpha_n - 1} + \frac{\cos(\alpha_n + 1)\theta}{\alpha_n + 1} - \frac{2\alpha_n}{\alpha_n^2 - 1} \right); \tag{3.21}$$

$$y(\theta) = \frac{1}{\gamma}\sum_{n=1}^{N} C_n \left(\frac{\sin(\alpha_n - 1)\theta}{\alpha_n - 1} - \frac{\sin(\alpha_n + 1)\theta}{\alpha_n + 1} \right). \tag{3.22}$$

All calculations were done using the mathematical package Maple V. Figure 3 shows boundaries of the bubble and respective stagnant zones. As it is seen from Fig. 4, even at large γ the elongated bubbles are almost elliptical.

3.3 Numerical-analytical solution for a power-law fluid

In this case, (2.2) becomes

$$\frac{1}{s}\frac{\partial}{\partial w}\left(w^s \frac{\partial \psi}{\partial w} \right) + w^{s-2}\frac{\partial^2 \psi}{\partial \theta^2} = 0. \tag{3.23}$$

https://doi.org/10.1017/S0956792504005509 Published online by Cambridge University Press

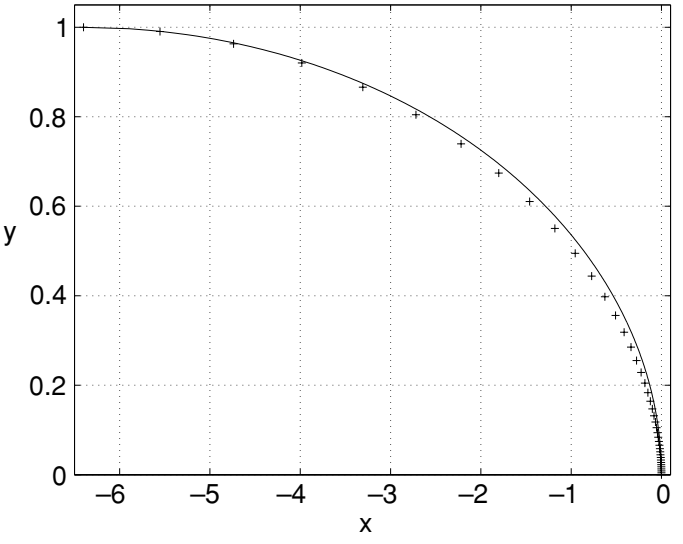

FIGURE 4. The shape of the bubble with $\gamma = 0.5$ (crosses) in comparison with an ellipse (solid line) of the same length; $V = 1$, $V_* = 0.9$.

The solution of (3.19) with the boundary conditions (see Figure 1)

$$\psi = 0 \quad \text{along} \quad AB \quad \text{and} \quad BC; \tag{3.24}$$

$$H = 0 \quad \left(\text{or} \quad \frac{\partial \psi}{\partial \theta} = 0\right) \quad \text{along} \quad CD; \tag{3.25}$$

$$0 \leqslant \theta \leqslant \pi, \qquad 0 \leqslant w \leqslant V, is\psi(u,\theta) = \sum_{n=1}^{\infty} C_n w^{k_n} \sin \alpha_n \theta, \tag{3.26}$$

$$k_n = \frac{1-s}{2} + \sqrt{\frac{(1-s)^2}{4} + s\alpha_n^2}. \tag{3.27}$$

The unknown coefficients C_n are determined using the collocation method from conditions on the bubble surface as stated above:

$$A(w,\theta)\frac{\partial \psi}{\partial w} + B(w,\theta)\frac{\partial \psi}{\partial \theta} = 0 \quad \text{along } AD; \tag{3.28}$$

$$\psi\left(\rho g^{1/s}, \pi\right) = \lambda V \quad \text{at the point } D. \tag{3.29}$$

Once more, the Saffman–Taylor solution corresponding to $s = 1$ was used as a benchmark (cf. Figures 5 and 6).

Figures 7–10 summarize the results. In Figures 7 and 8, the bubble aspect ratio (length-to-width ratio) and relative area are presented as functions of the bubble velocity for different values of γ. Both the aspect ratio and the rate of its growth with velocity increase with increasing γ (i.e. the plastic component of flow resistance). Briefly, in a Bingham fluid the bubbles prove to be more elongated. The same qualitative behaviour is observed

https://doi.org/10.1017/S0956792504005509 Published online by Cambridge University Press

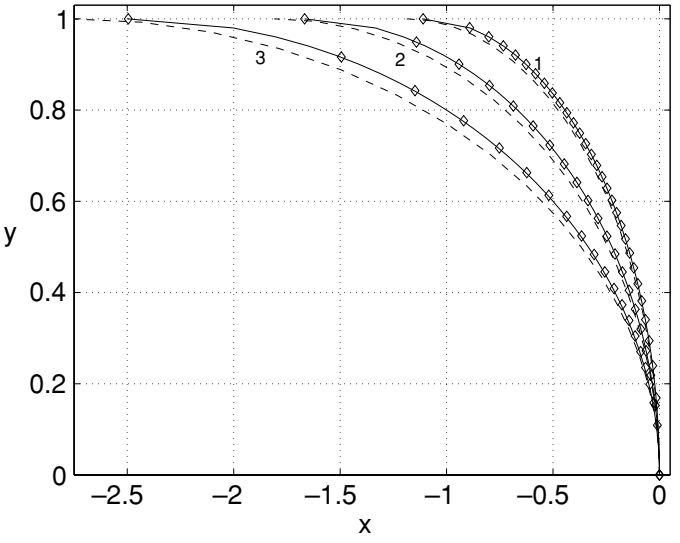

FIGURE 5. The bubble shapes derived by the collocation technique at different V_* for a power-law fluid for $s = 1$ (diamonds), flow with limiting pressure gradient with $\gamma = 0.01$ (broken lines). Solid lines correspond to the Saffman–Taylor solution. 1: $V_* = 0.9$, 2: $V_* = 0.6$, 3: $V_* = 0.4$.

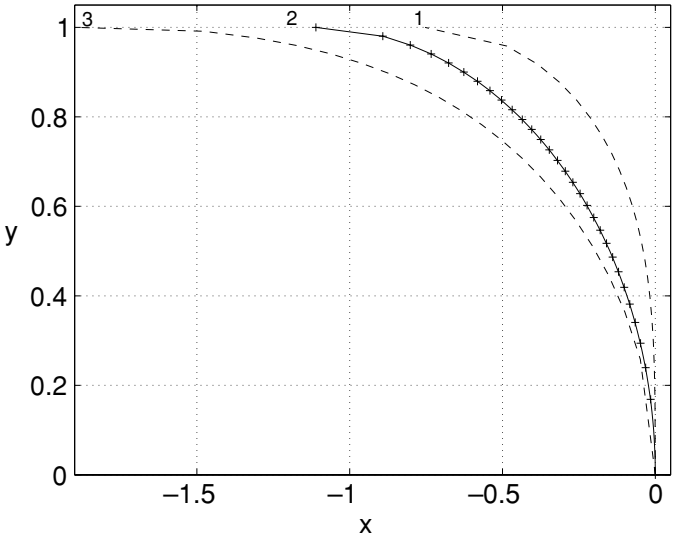

FIGURE 6. The bubble shape for power-law fluids derived by the collocation technique for $s = 1$ (crosses) $s = 0.7$ – broken line (1), $s = 3$ – broken line (3), the Saffman–Taylor solution is shown by a solid line.

for power-law shear-thinning fluids ($s < 1$). Notice (Figures 9 and 10), that in this formal theory the bubble velocity and thickness λ are both free parameters, and for given bubble area there exists a family of bubbles of different aspect ratio, the bubble velocity being the greater the greater the aspect ratio.

https://doi.org/10.1017/S0956792504005509 Published online by Cambridge University Press

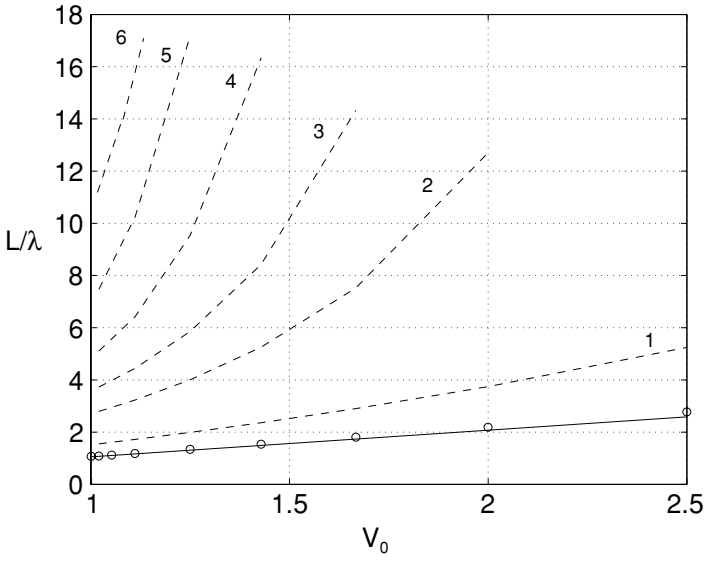

FIGURE 7. The bubble aspect ratio (the length-to-width ratio), *vs* dimensionless velocity, $V_0 = 12\eta V/\rho g b^2$. The solid line shows the Saffman–Taylor solution, circles and broken lines correspond to flow with limiting pressure gradient at different γ derived by the collocation technique. The respective values are: $\gamma = 0.005$ (circles), $\gamma = 0.1$ (curve 1), $\gamma = 0.3$ (curve 2), $\gamma = 0.4$ (curve 3), $\gamma = 0.5$ (curve 4), $\gamma = 0.6$ (curve 5), $\gamma = 0.7$ (curve 6).

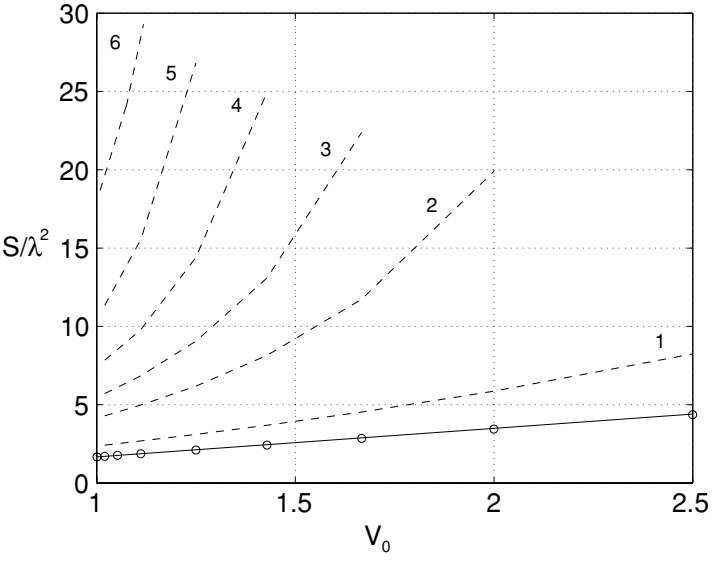

FIGURE 8. The bubble relative area *vs* dimensionless velocity, $V_0 = 12\eta V/\rho g b^2$. The solid line shows the Saffman–Taylor solution, circles and broken lines correspond to flow with limiting pressure gradient at different γ derived by the collocation technique. The respective values are: $\gamma = 0.005$ (circles), $\gamma = 0.1$ (curve 1), $\gamma = 0.3$ (curve 2), $\gamma = 0.4$ (curve 3), $\gamma = 0.5$ (curve 4), $\gamma = 0.6$ (curve 5), $\gamma = 0.7$ (curve 6).

https://doi.org/10.1017/S0956792504005509 Published online by Cambridge University Press

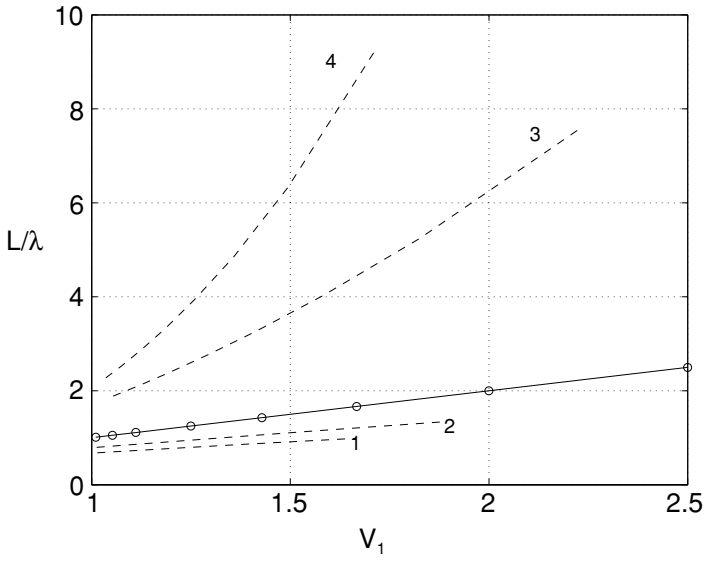

FIGURE 9. The bubble aspect ratio (length-to-width ratio). The solid line shows the Saffman–Taylor solution, circles and broken lines correspond to power-law fluid at different s derived by the collocation technique. The respective values are: $s = 1$ (circles), $s = 0.7$ (curve 1), $s = 0.8$ (curve 2), $s = 2$ (curve 3), $s = 3$ (curve 4).

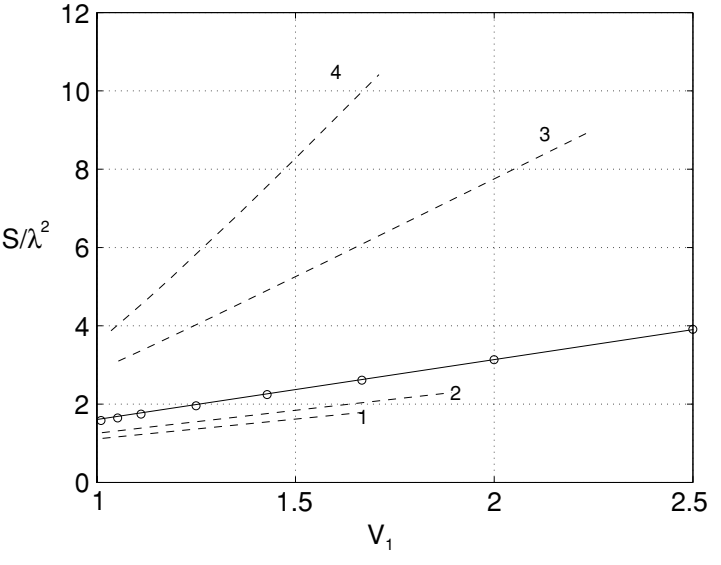

FIGURE 10. The bubble dimensionless area *vs* dimensionless velocity. The solid line shows the Saffman–Taylor solution, circles and broken lines correspond to power-law fluid at different s derived by the collocation technique. The respective values are: $s = 1$ (circles), $s = 0.7$ (curve 1), $s = 0.8$ (curve 2), $s = 2$ (curve 3), $s = 3$ (curve 4).

https://doi.org/10.1017/S0956792504005509 Published online by Cambridge University Press

4 Conclusion

A combined analytical-numerical technique was developed to treat the problem of an inviscid bubble rising due to buyoancy through an unbounded Hele–Shaw cell filled with a nonlinearly viscous fluid. Results are presented for the cases of a Bingham and power-law fluids. In the limiting case of a Newtonian fluid these results agree rather well with benchmark solution due to Saffman and Taylor. In all cases, for given bubble area a one-parameter family of solutions is derived differing in the bubble shape and rising velocity. The bubbles aspect ratio increases with velocity, the rate of increase being greater for Bingham and shear-thinning fluids than for a Newtonian fluid.

The technique can be extended to many related problems of plane flows with free boundaries following a nonlinear flow rule.

References

[1] Alexandrou, A. N. & Entov, V. M. (1997) On the steady-state advancement of fingers and bubbles in a Hele-Shaw cell filled by a non-Newtonian fluid. *Euro. J. Appl. Math.* **8**, 73–87.

[2] Barenblatt, G. I., Entov, V. M. & Ryzhik, V. M. (1990) *Fluids Flow through Natural Rocks.* Kluwer.

[3] Bernadiner, M. G. & Entov, V. M. (1975) *Hydrodynamical Theory of Flow of Anomalous Fluids through Porous Media.* Nauka, Moscow (in Russian).

[4] Bernadiner, M. G., Entov, V. M. & Turetskaya F. D. (1974) *The numerical solution of steady-state problems of nonlinear seepage*. Moscow, Preprint in the IPM publ. (in Russian).

[5] Bonn, D., Kellay, H., Ben Amar, M. & Meunier, J. (1995) Viscous finger widening with surfactants and polymers. *Phys. Rev. Lett*. **75**, 2132.

[6] Goldstein, R. V. & Entov, V. M. (1994) *Qualitative Methods in Continuum Mechanics,* Pitman Monographs and Surveys in Applied Mathematics, Longman.

[7] Kondic, L., Palffy-Muhoray, P. & Shelley, M. J. (1996) Models of non-Newtonian Hele-Shaw flow. *Phys. Rev. E*, **54**(5), R5436–R5439.

[8] Lebedev, N. N. (1965) *Special Functions and their Applications.* Prentice Hall.

[9] Reiner, M. (1949) *Deformation and Flow, an Elementary Introduction to Theoretical Rheology*. H. K. Lewis, London.

[10] Saffman, P. G. & Taylor, G. I. (1958) The penetration of a fluid into a porous medium or Hele-Shaw cell containing a more viscous liquid. *Proc. Roy. Soc. Lond.* **A 245**, 312–329.

[11] Saffman, P. G. & Taylor, G. I. (1959) A note on the motion of bubbles in a Hele-Shaw cell and porous medium. *Q. J. Mech. Appl. Math.* **12**, 265–279.

[12] Kondic, L., Shelley, M. J. & Palffy-Muhoray, P. (1998) Non-Newtonian Hele-Shaw flow and the Saffman-Taylor instability. *Phys. Rev. Lett*. **80**(7), 1433–1436.

[13] Ianenko, N. N. (1971) *The Method of Fractional Steps; the Solution of Problems of Mathematical Physics in Several Variables* . Springer-Verlag.